A Waveguide Mode-Converter Feed for a 5-W, 34-GHz Grid Amplifier

Chun-Tung Cheung[1], Jonathan B. Hacker[2], Gabor Nagy[2], David B. Rutledge[1]
[1]California Institute of Technology, Pasadena, CA
[2]Rockwell Scientific Company LLC, Thousand Oaks, CA

Abstract— **We have demonstrated a compact waveguide mode converter that excites a combination of TE_{10} and TE_{30} modes for feeding a grid amplifier. The length of the mode converter is only 13mm. The effective transmitter power (ETP) at 34GHz is 5W, with a gain of 5.5dB and a power-added efficiency (PAE) of 21%. The supply voltage is 3V, with a bias current of 5.6A. These results are comparable to those reported earlier for the same grid-amplifier design measured in free space. A spurious oscillation with a broad radiation pattern was observed at 33.6GHz with an effective isotropic radiated power (EIRP) of 23mW. This oscillation was suppressed when the grid was operating at high power levels, and disappeared entirely at output powers above 4.5W.**

I. Introduction

Quasi-optical amplifiers have demonstrated the capability of combining the power of several hundred transistors with multi-watt output at millimeter-wave frequencies [1]-[3]. Traditional spatial-power-combining grid amplifiers use a gaussian focused-beam system for measurements. Gaussian-beam systems give excellent phase and amplitude distributions but use very large lenses. Therefore, new compact packaging techniques were sought to solve the problem. In [3] and [4], tapered-waveguide feeds, of length 230mm and 75mm respectively, excited the amplifiers. However, these tapered feeds are long, and in [4], there were rapid gain fluctuations with frequency because of multiple reflections of higher-order modes along the long taper. Ali *et al.* [5] successfully demonstrated a hard-wall waveguide horn to feed a hybrid spatial-power-combining amplifier with 10-dB gain at 25-W output power. Kim *et al.* [6] proposed an ingenious feed using a TEM waveguide with photonic-crystal walls, but this has not yet been demonstrated with an amplifier.

In this paper, we show the design and construction of a waveguide mode-converter feed that drives a grid amplifier. When fed by the mode converter, the grid amplifier gives power, gain and efficiency comparable to that reported earlier for a gaussian-beam feed [1]. The mode converter is only 13mm long and would be suitable for inexpensive fabrication. It allows the output amplified signal to radiate into free space in a beam that would be appropriate for illuminating a parabolic dish antenna.

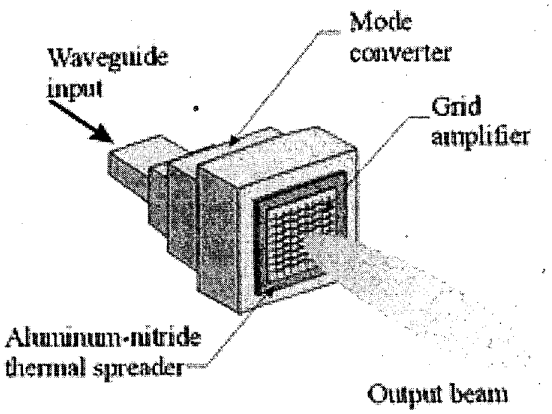

Fig. 1. The schematic of the waveguide feed grid amplifier.

II. Design

The mode converter is a structure cascading two sections of metal waveguide of different sizes. Metal waveguide is used because it provides low loss and high thermal conductivity. The input is a standard WR28 waveguide and the output is a rectangular over-moded waveguide of 13mm ×11mm. The active area of the grid is a 10-mm square [1]. In order to design the waveguide structure, Matlab Nelder-Mead optimization together with Ansoft HFSS simulation was used.

We first design a passive port-to-port mode converter for field probing. This is done by optimizing the dimensions of the waveguide sections to minimize input return loss, set the field magnitude ratio between TE_{30} and TE_{10} modes to 0.28 and suppress any other higher order modes travelling in over-moded waveguide. This field ratio results in a 2-dB ripple in the H-plane at equal phase planes across 70% of the waveguide width. The minimization function is

$$e = |S11|^2 + \left(0.28 - \frac{|S21_{TE30}|}{|S21_{TE10}|}\right)^2 + \sum_{higher\ order} |S21_{TE}|^2 + \sum_{all\ modes} |S21_{TM}|^2 \quad (1)$$

The two travelling modes have different phase velocity,

0-7803-7239-5/02/$10.00 © 2002 IEEE

the specified spatial distribution only occurs when the phases are equal.

The passive mode-converter design is then used as an initial guess for the active mode converter shown in Fig. 1. This design includes the effect of thermal spreader, the gallium-arsenide substrate and the DC-bias circuitry. The mode converter dimensions are subject to a new minimization function

$$e = |S11|^2 + \Delta^2 + \delta^2 \qquad (2)$$

where Δ is the standard deviation of the normalized amplitude, and δ is the standard deviation of the phase in radians. Initial guesses of tuning-slug thickness and separations can be obtained from traditional circuit simulation with fundamental-mode transmission-line models. The modeling of the unit cell of the grid amplifier follows Preventza *et al.* [7]. The input impedance of the amplifier can then be obtained and the grid can be modelled as an impedance sheet. Since the output impedance varies during optimization, a lookup table of input impedance of the amplifier with different tuning slug thicknesses and separations was generated. When the optimizer specifies the new dimensions, it checks the corresponding impedance from the table with the help of linear interpolation. Eventually, the optimized results are applied to circuit simulation to verify the output matching. For the optimized structure, the input return loss is 16dB, $\Delta = 0.11$, and $\delta = 6.4°$.

III. Measurement

We first tested the passive mode converter without amplifier using monopole and loop probes. The probing technique was the same as described in [8], which describes an earlier different tapered mode converter. The probe fields in the E and H planes are shown in Fig. 2 at the uniform-phase plane. The measured return loss 20-dB bandwidth is 10% which implies the passive mode converter does not impose major bandwidth reduction (Fig 3).

The mode converter for mounting the amplifier chip was then fabricated. The input-side polarizer was fabricated by etching a pattern in copper sheet. Shims of various thicknesses were used for adjusting the tuning of the amplifier by the input-side polarizer. The output-side polarizer is patterned on a piece of Duroid 0.254 mm thick with a dielectric constant of 10.2. An additional Duroid tuning slab with a dielectric constant of 2.2 was added behind the output-side polarizer. The thermal spreader, made from aluminum nitride, was held against the waveguide wall by making use of the difference in thermal expansion of brass and aluminum nitride. The amplifier chip was then glued onto this thermal spreader.

For radiated output power and amplifier gain, we use

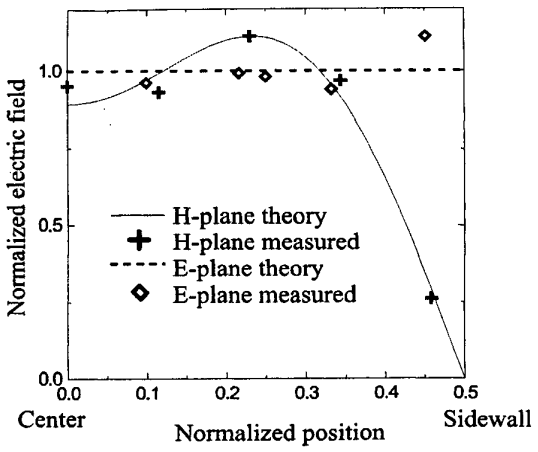

Fig. 2. The probed field distribution of mode converter at uniform phase plane. The technique is described in [8] E-plane distribution was measured with loop probe while H-plane distribution measured with monopole probe.

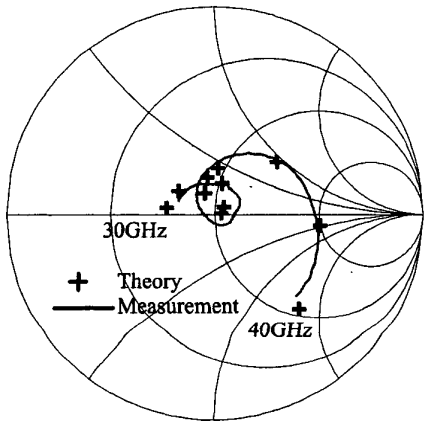

Fig. 3. Simulated and measured return loss of the passive mode converter with no amplifier present. The return loss is greater than 20dB over a 10% bandwidth.

the effective transmitter power (ETP) and system gain defined by Gouker[9]. The geometric area of the grid, 100mm^2, was used for normalization. The maximum small-signal gain is 7.5dB at 34.4GHz with a 5% 3-dB bandwidth (Fig. 4). The measured and calculated input return loss are also shown on the same plot. The system gain of the amplifier and power-added efficiency (PAE) are measured at 34.4GHz and plotted against ETP in Fig. 5. The maximum PAE is 22% at 5.4W ETP and 5.5dB gain. A normalized radiation pattern was measured at 34.4GHz with 3-dB gain compression

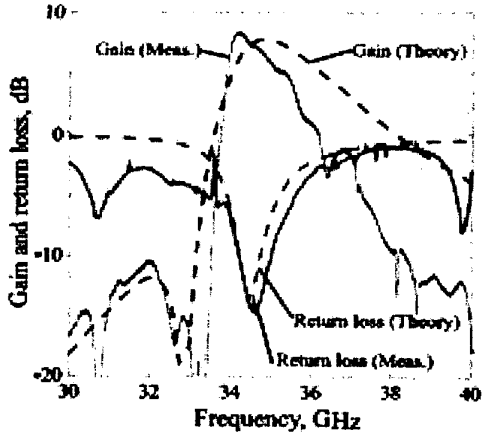

Fig. 4. Simulated and measured small-signal gain and return loss. The geometric area is used for gain normalization.

and 5.5W ETP for E and H-plane (Fig. 6). A 13-mm uniform aperture and a finite-difference time-domain (FDTD) simulation radiation patterns are plotted on Fig. 6 for comparison. The fitted radiation aperture is bigger than the active grid area, and it implies that gain and ETP may be optimistic when the geometric area is used for normalization. The FDTD simulation with anisotropic material modelled grid amplifier suggested that the effective radiation area is bigger than geometric area. The ETP and gain are correspondingly decreased by 2dB while the input power remains the same. The third-order intermodulation was measured at 34.4GHz with 10-MHz separation between the two carrier tones, and the carrier to intermodulation ratio is plotted in Fig. 7. The calculated third-order intercept from the measured data is 5W. The measured AM-to-PM conversion is 10°/W (Fig. 8).

There were spurious oscillations at 33.6GHz with an EIRP of 23mW (Fig. 9). The radiation patterns of the oscillation are quite broad and we think the oscillation is a common-mode oscillation described in [11]. We suspect that we need a bigger common-mode stability factor in order to avoid oscillation due to process and mounting variations. The spurious oscillation is compressed at high power and is completely eliminated for powers above 4.5W.

IV. Conclusions

We have demonstrated a waveguide mode converter with a length of only 13mm for feeding a 5-W Ka-band grid-amplifier. The power, efficiency, and gain were similar to those reported for the same grid amplifier design with free-space measurements (Table 1). The third-order intermodulation and AM-to-PM conversion are considerably worse for the waveguide feed and we do not know the reason for this. This is a first step toward integrating grid amplifiers into a waveguide system.

	Free-space	Waveguide
Drain voltage, V	2.7	3
Drain current, A	6.5	5.6
Freq, GHz	37	34
Small signal gain, dB	8	7.5
Gain at 5-W output, dB	5	5.7
3-dB BW, %	3.5	5
PAE at 5-W output, %	17	21
3rd-order intercept, W	32	5
AM-PM conversion, °/W	4	10

Table 1. Comparison of free-space gaussian-beam and waveguide mode converter measurements. The free-space data are taken from [1] and [10]. The geometric area is used for normalization.

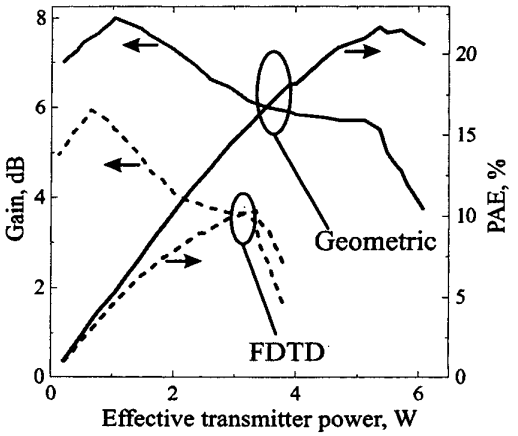

Fig. 5. Measured gain and power-added efficiency (PAE) versus output effective transmitter power (ETP) at 34.4GHz. Solid lines are normalized by the geometric area and dotted lines are normalized by the effective area predicted by finite-difference time-domain simulation.

Acknowledgement The authors appreciate the support from the Army Research Office through the Caltech Quasi-Optic Power Combining MURI program.

References

[1] B. Dickman, D. S. Deakin, Jr., E. Sovero, D. Rutledge, "A 5-Watt, 37-GHz Monolithic Grid Amplifier," 2000 Int. Microwave Symp. Dig., pp. 805-808.

[2] B. Dickman, J. J. Rosenberg, D. Rutledge, E. Sovero, D. S. Deakin, Jr., "A 1-Watt, 38-GHz Monolithic Grid Oscillator," 2001 Int. Microwave Symp. Dig., pp. 1843-1846.

[3] J. J. Sowers, D. J. Pritchard, A. E. White, W. Kong, O.S.A. Tang, D. R. Tanner and K. Jablinskey, "A 36W, V-Band, Solid State Source," 1999 Int. Microwave Symp. Dig., pp. 235-238.

[4] E. A. Sovero, J. B. Hacker, J. A. Higgins, D. S. Deakin, and A. L. Sailer, "A Ka-band Monolithic Quasi-Optic Amplifier," 1998 Int. Microwave Symp. Dig., pp. 1453-1456.

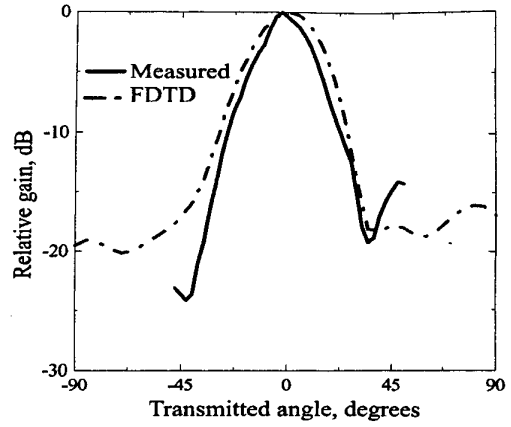

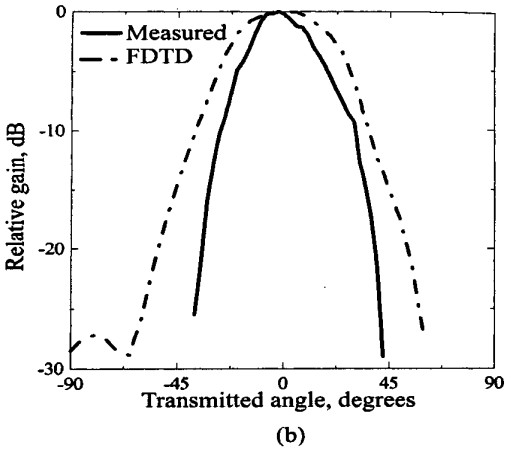

Fig. 6. Measured and FDTD predicted radiation pattern. (a) E-plane (b) H-plane.

[5] S. Ortiz, J. Hubert, L. Mirth, E. Schlecht, and A. Mortazawi, "A 25 Watt and 50 Watt Ka-band Quasi-Optical Amplifier," 2000 In. Microwave Symp. Dig., pp. 797-800.

[6] M. Kim, J. B. Hacker, A. L. Sailor, S. Kim, D. Sievenpiper and J. A. Higgins, "A Rectangular TEM Waveguide and Photonic Crystal Walls For Excitation of Quasi-Optical Amplifiers," 1999 Int. Microwave Symp. Dig., pp. 543-546.

[7] P. Preventza, B. Dickman, E. Sovero, M. P. DeLisio, J. J. Rosenberg, D. B. Rutledge, "Modeling of Quasi-Optical Arrays," 1999 Int. Microwave Symp. Dig., pp. 563-566.

[8] T. Kamei, H. Morishita, C-T Cheung, D. B. Rutledge, "Design of a Mode Converter for Quasi-Optical Amplifiers by Using 3D EM Simulation Software," *IEICE Trans. Electron.*, Vol. E84-C, 2001, pp. 955-960.

[9] M. A. Gouker, "Toward Standard Figures-of-merit for Spatial and Quasi-optical Array," *IEEE Trans. Microwave Theory Tech.*, vol. 43, 1995, pp. 1614-1617.

[10] J. Harvey, E. R. Brown, D. B. Rutledge, R. A. York, "Spatial Power Combining for High-Power Transmitters," *IEEE Microwave Magazine*, vol. 1, 2000, pp. 48-59.

[11] C. M. Liu, M. P. DeLisio, A. Moussessian, D. B. Rutledge, "Stability of Grid Amplifiers," *IEEE Trans. Microwave Theory Tech.*, vol. 46, 1998, pp. 769-774.

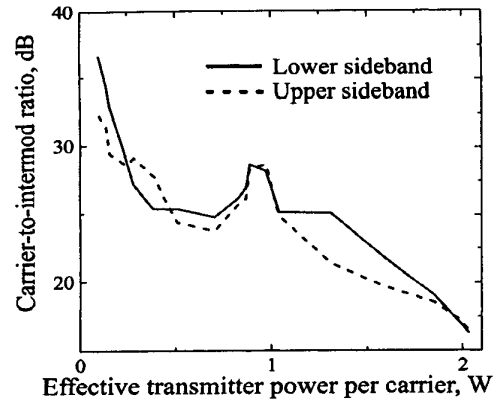

Fig. 7. The third-order intermodulation measurement. The third-order intercept is 5W ETP. The geometric area is used for normalization.

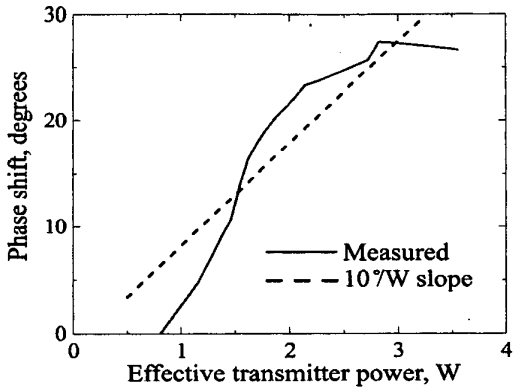

Fig. 8. Measured and fitted AM-to-PM conversion. A line with a 10°/W slope is shown for comparison. The geometric area is used for normalization.

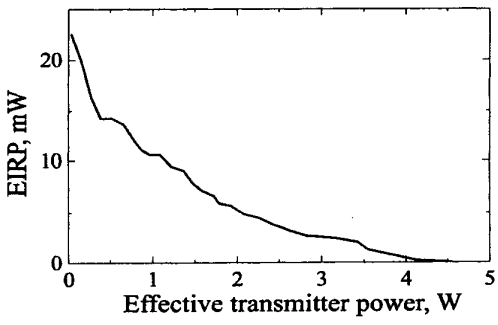

Fig. 9. Effective isotropic radiated power (EIRP) of spurious oscillation at 33.6GHz, plotted against carrier output power. The oscillation is suppressed at high output powers.